

Ca²⁺ shuttling between endoplasmic reticulum and mitochondria underlying Ca²⁺ oscillations

Kiyoaki Ishii¹, Kenzo Hirose^{1,2} & Masamitsu Iino^{1*}

¹Department of Pharmacology, Graduate School of Medicine, The University of Tokyo, Bunkyo-ku, Tokyo, Japan, and ²Department of Cell Physiology, Nagoya University Graduate School of Medicine, Showa-Ku, Nagoya, Japan

Although many cell functions are regulated by Ca²⁺ oscillations induced by a cyclic release of Ca²⁺ from intracellular Ca²⁺ stores, the pacemaker mechanism of Ca²⁺ oscillations remains to be explained. Using green fluorescent protein-based Ca²⁺ indicators that are targeted to intracellular Ca²⁺ stores, the endoplasmic reticulum (ER) and mitochondria, we found that Ca²⁺ shuttles between the ER and mitochondria in phase with Ca²⁺ oscillations. Following agonist stimulation, Ca²⁺ release from the ER generated the first Ca²⁺ oscillation and loaded mitochondria with Ca²⁺. Before the second Ca²⁺ oscillation, Ca²⁺ release from the mitochondria by means of the Na⁺/Ca²⁺ exchanger caused a gradual increase in cytoplasmic Ca²⁺ concentration, inducing a regenerative ER Ca²⁺ release, which generated the peak of Ca²⁺ oscillation and partially reloaded the mitochondria. This sequence of events was repeated until mitochondrial Ca²⁺ was depleted. Thus, Ca²⁺ shuttling between the ER and mitochondria may have a pacemaker role in the generation of Ca²⁺ oscillations.

Keywords: calcium oscillation; endoplasmic reticulum; GFP; imaging; mitochondria

EMBO reports (2006) 7, 390–396. doi:10.1038/sj.embor.7400620

INTRODUCTION

Ca²⁺ oscillation is a periodic spiking of intracellular Ca²⁺ concentration observed in many types of cell under stimulation (Clapham, 1995; Berridge *et al*, 2000), and Ca²⁺-dependent molecules are often regulated by the frequency of Ca²⁺ oscillations (De Koninck & Schulman, 1998; Dolmetsch *et al*, 1998; Li *et al*, 1998; Oancea & Meyer, 1998; Tomida *et al*, 2003). Although the importance of Ca²⁺ oscillations is widely recognized, the mechanism underlying Ca²⁺ oscillations remains to be explained. In many cell types, Ca²⁺ release by means of the

inositol 1,4,5-trisphosphate receptor (IP₃R) has a pivotal role in the generation of Ca²⁺ oscillations. The IP₃R function is regulated not only by IP₃ concentration, but also by cytoplasmic Ca²⁺ concentration (Iino, 1990; Bezprozvanny *et al*, 1991). The Ca²⁺-mediated regulation of IP₃R is essential for Ca²⁺ oscillations, because cells expressing a mutant IP₃R with a reduced sensitivity to Ca²⁺ do not generate Ca²⁺ oscillations (Miyakawa *et al*, 2001). Although the endoplasmic reticulum (ER), which carries IP₃R, is mainly responsible for the generation of Ca²⁺ oscillations, mitochondria may also have a role as a buffer of cytoplasmic Ca²⁺ concentration (Jouaville *et al*, 1995; Rizzuto *et al*, 1998). However, the functions of these organelles in the generation of Ca²⁺ oscillations require further clarification.

We measured Ca²⁺ concentration dynamics within intracellular Ca²⁺ stores simultaneously with cytoplasmic Ca²⁺ concentration using green fluorescent protein (GFP)-based Ca²⁺ indicators that were designed to monitor Ca²⁺ concentration within either the ER or mitochondria. Our results show that Ca²⁺ concentrations in both ER and mitochondria oscillate concomitantly with cytoplasmic Ca²⁺ oscillations. There are, however, important phase differences in oscillatory change among the three compartments. Our results indicate that Ca²⁺ shuttling between the ER and mitochondria is an essential component of the Ca²⁺ oscillation mechanism, and has a pacemaker role in Ca²⁺ oscillations.

RESULTS AND DISCUSSION

Ca²⁺ measurement within ER

To monitor Ca²⁺ concentration inside the ER ([Ca²⁺]_{er}), we used the GFP-based Ca²⁺ indicator (cameleon) after modifications (split-YC7.3er, K'_d ≈ 130 μM; see supplementary information and supplementary Fig 1 online). We examined whether the indicator detects [Ca²⁺]_{er} in living cells. HeLa cells were sequentially transduced with retroviruses that encode the two parts of the indicator, and both parts were expressed in the cytoplasmic meshwork structure of the ER (supplementary Fig 2 online). On application of histamine, F480 increased, with a concomitant decrease in F535, as expected from a decrease in [Ca²⁺]_{er} (Fig 1A, upper diagram). We used F₅₃₅/F₄₈₀ as an indicator of [Ca²⁺]_{er} (Fig 1A, lower diagram). After histamine application, F₅₃₅/F₄₈₀ decreased without any noticeable delay after the increase in

¹Department of Pharmacology, Graduate School of Medicine, The University of Tokyo, Bunkyo-ku, Tokyo 113-0033, Japan

²Department of Cell Physiology, Nagoya University Graduate School of Medicine, Showa-Ku, Nagoya 466-8550, Japan

*Corresponding author. Tel: +81 3 5841 3417; Fax: +81 3 5841 3390;

E-mail: iino@m.u-tokyo.ac.jp

Received 20 June 2005; revised 22 November 2005; accepted 30 November 2005; published online 13 January 2006

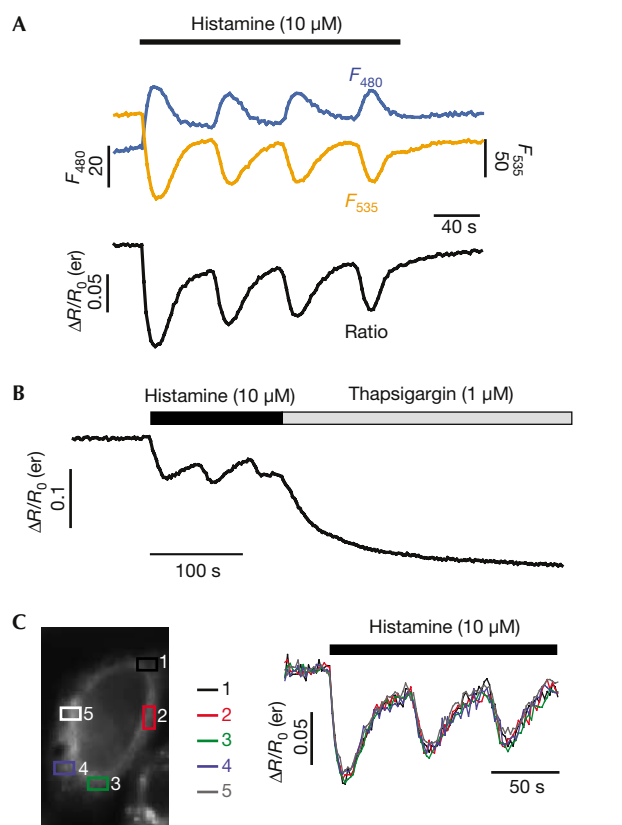


Fig 1 | Measurement of $[\text{Ca}^{2+}]_{\text{er}}$ using split-YC7.3er. (A) Fluorescence change in a cell expressing split-YC7.3er cameleon after histamine stimulation. Fluorescence intensities (434 nm excitation) at 535 (F_{535}) and 480 nm (F_{480} ; upper diagram) and their ratio F_{535}/F_{480} (lower diagram). (B) Time course of F_{535}/F_{480} during application of histamine and thapsigargin. Data are representative of five experiments. (C) Time courses of F_{535}/F_{480} at different areas within the cell shown in the left panel. Data are representative of four experiments.

cytoplasmic Ca^{2+} concentration ($[\text{Ca}^{2+}]_{\text{cyt}}$; Fig 2A,C,E,F), indicating that the indicator is not saturated with a luminal Ca^{2+} concentration in the resting state. When ER Ca^{2+} was subsequently depleted by inhibiting sarco(endo)plasmic reticulum Ca^{2+} ATPase (SERCA) by thapsigargin, F_{535}/F_{480} decreased below the trough of histamine-induced oscillatory changes (Fig 1B). These results indicate that the dynamic range of split-YC7.3er covers the entire range of changes in $[\text{Ca}^{2+}]_{\text{er}}$ during histamine-induced Ca^{2+} oscillations. We did not observe any distinct spatial inhomogeneity in $[\text{Ca}^{2+}]_{\text{er}}$ measurements within cells at the present time resolution (Fig 1C).

$[\text{Ca}^{2+}]_{\text{cyt}}$ versus $[\text{Ca}^{2+}]_{\text{er}}$

We then carried out simultaneous measurements of $[\text{Ca}^{2+}]_{\text{cyt}}$ and $[\text{Ca}^{2+}]_{\text{er}}$ using indo-5F and split-YC7.3er, respectively. As shown in Fig 2A, histamine induced oscillatory changes in $[\text{Ca}^{2+}]_{\text{cyt}}$ and $[\text{Ca}^{2+}]_{\text{er}}$ in opposite directions. Ca^{2+} oscillations were also observed in the absence of the extracellular Ca^{2+} (Fig 2C). The following analyses mainly use data in the absence of extracellular Ca^{2+} , because the absence of Ca^{2+} influx through the plasma membrane simplifies the analyses.

Fig 2E shows the very first Ca^{2+} oscillation in response to histamine application. $[\text{Ca}^{2+}]_{\text{cyt}}$ increased rapidly, reaching a peak in ~ 4 s. Conversely, the $[\text{Ca}^{2+}]_{\text{er}}$ change had the same onset time as the $[\text{Ca}^{2+}]_{\text{cyt}}$ change, but $[\text{Ca}^{2+}]_{\text{er}}$ continued to decrease after $[\text{Ca}^{2+}]_{\text{cyt}}$ reached its peak. The time courses of $[\text{Ca}^{2+}]_{\text{er}}$ and $[\text{Ca}^{2+}]_{\text{cyt}}$ during the first oscillations in different experiments were averaged after normalization (Fig 2F; see the supplementary information online for normalization procedure). The main features of the typical data are discernible in the averaged data. Thus, at the peak $[\text{Ca}^{2+}]_{\text{cyt}}$, only $41.5 \pm 10.7\%$ (mean \pm s.d., $n = 13$) of the full $[\text{Ca}^{2+}]_{\text{er}}$ response was reached. After $[\text{Ca}^{2+}]_{\text{cyt}}$ reached its peak, Ca^{2+} release from the ER continued for ~ 10 s (9.9 ± 1.7 s, mean \pm s.d., $n = 13$). This suggests that a significant fraction of Ca^{2+} released from the ER enters non-ER Ca^{2+} stores or exits the cell without further increasing $[\text{Ca}^{2+}]_{\text{cyt}}$. The apparent delay of $[\text{Ca}^{2+}]_{\text{er}}$ signal amounting to ~ 10 s cannot be due to the response time of the indicator, because the off rate constant of cameleon is $\sim 13 \text{ s}^{-1}$ (Miyawaki *et al*, 1997); indeed, there was no noticeable lag time at the onset of the first Ca^{2+} oscillation (Fig 2E,F).

The second and subsequent Ca^{2+} oscillations showed a different time course. The rate of increase in $[\text{Ca}^{2+}]_{\text{cyt}}$ was much lower than that of the initial spike (Fig 2D versus Fig 2E). We discerned three phases in Ca^{2+} dynamics, as indicated by the shaded boxes in Fig 2D. In phase 1 (from the bottom of $[\text{Ca}^{2+}]_{\text{cyt}}$ to the initiation of Ca^{2+} release from the ER), $[\text{Ca}^{2+}]_{\text{cyt}}$ increased, generating the foot of Ca^{2+} oscillation. Unexpectedly, $[\text{Ca}^{2+}]_{\text{er}}$ rather increased (that is, the ER was taking up Ca^{2+}) during phase 1. As there was no entry of Ca^{2+} from the extracellular space, Ca^{2+} must be supplied from non-ER Ca^{2+} stores to generate the foot of Ca^{2+} oscillation. In phase 2 (the falling phase of $[\text{Ca}^{2+}]_{\text{er}}$), ER Ca^{2+} was released, increasing $[\text{Ca}^{2+}]_{\text{cyt}}$. During late phase 2, Ca^{2+} release from the ER continued, but $[\text{Ca}^{2+}]_{\text{cyt}}$ started to decrease after reaching a peak. This indicates that Ca^{2+} released from the ER is entering non-ER Ca^{2+} stores or leaving the cell. In phase 3 (from the bottom of $[\text{Ca}^{2+}]_{\text{er}}$ to the bottom of $[\text{Ca}^{2+}]_{\text{cyt}}$), $[\text{Ca}^{2+}]_{\text{cyt}}$ decreased, whereas $[\text{Ca}^{2+}]_{\text{er}}$ increased, returning to the pre-oscillation level. Essentially the same patterns were detected in the presence of extracellular Ca^{2+} (Fig 2B).

The time courses of $[\text{Ca}^{2+}]_{\text{er}}$ and $[\text{Ca}^{2+}]_{\text{cyt}}$ during the second and third oscillations in different experiments were averaged after normalization. The main features of the aforementioned typical data are discernible in the averaged data, and Ca^{2+} release from the ER lags significantly after the increase in $[\text{Ca}^{2+}]_{\text{cyt}}$ at the onset of the third Ca^{2+} oscillation (Fig 2G).

$[\text{Ca}^{2+}]_{\text{cyt}}$ versus $[\text{Ca}^{2+}]_{\text{mt}}$

The above results indicate that non-ER Ca^{2+} stores have an important role in Ca^{2+} dynamics during Ca^{2+} oscillations: releasing Ca^{2+} in phase 1 and absorbing Ca^{2+} in phase 2. Mitochondria function as a Ca^{2+} buffer, taking up Ca^{2+} released from the ER (Jouaville *et al*, 1995; Babcock *et al*, 1997). Thus, mitochondria may be the non-ER Ca^{2+} store involved in Ca^{2+} oscillations. We therefore examined intramitochondrial Ca^{2+} concentration ($[\text{Ca}^{2+}]_{\text{mt}}$), using one of the circular permutation-type GFP-based Ca^{2+} indicators (inverse-pericam; Nagai *et al*, 2001) after modification. The indicator inverse-pericam2-mt carries a mitochondrial-targeting signal sequence at the amino-terminus and Citrine mutation. Calibrations using the recombinant protein at pH 8.0 (mimicking the mitochondrial environment; see

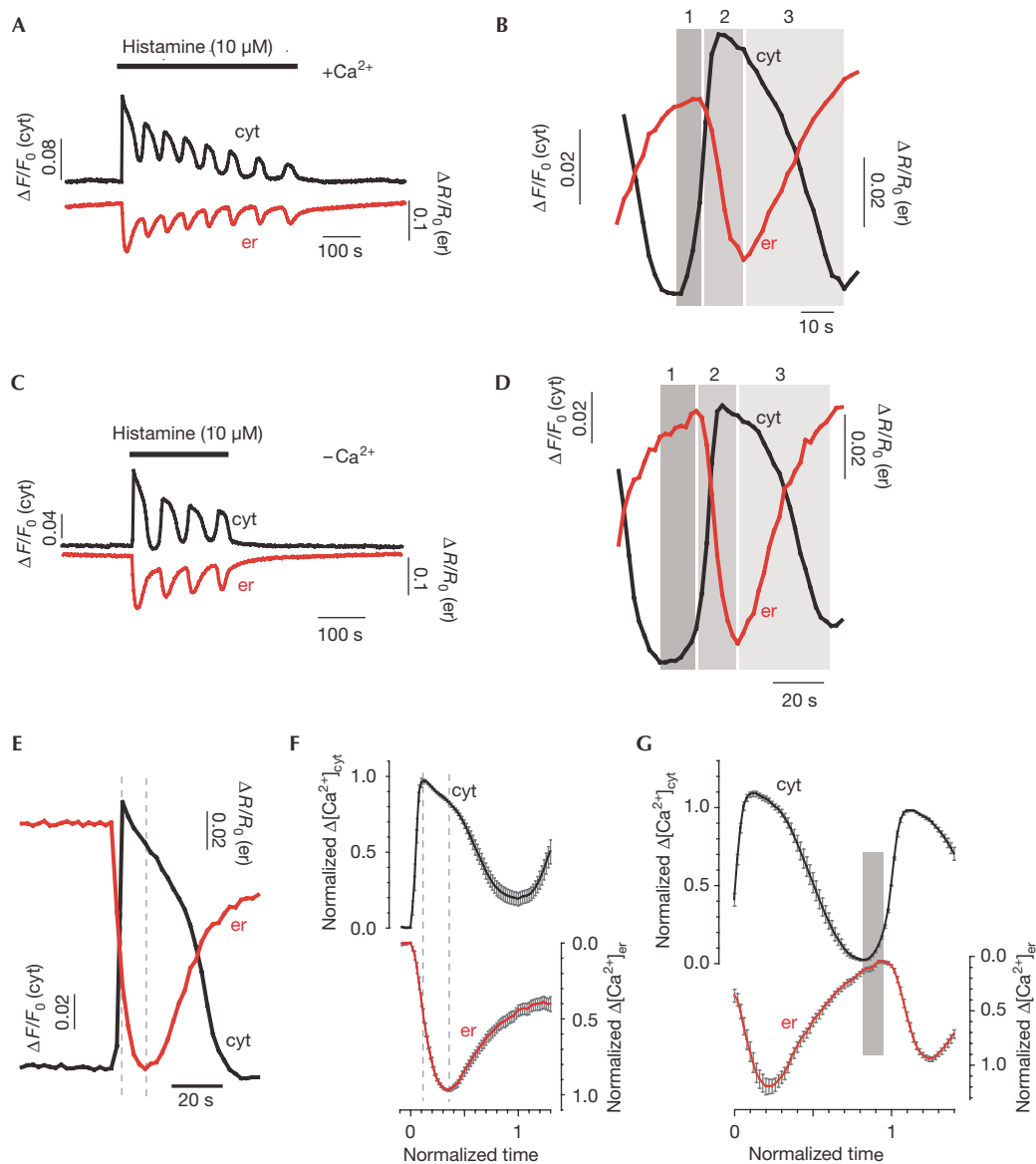


Fig 2 | Phase difference between $[\text{Ca}^{2+}]_{\text{er}}$ and $[\text{Ca}^{2+}]_{\text{cyt}}$. (A) Simultaneous measurement of $[\text{Ca}^{2+}]_{\text{er}}$ and $[\text{Ca}^{2+}]_{\text{cyt}}$ using split-YC7.3er cameleon and indo-5F, respectively, during histamine application in the presence of extracellular Ca^{2+} (2 mM). Data are representative of ten experiments. (B) Expanded time courses of $[\text{Ca}^{2+}]_{\text{er}}$ and $[\text{Ca}^{2+}]_{\text{cyt}}$ of second Ca^{2+} oscillation in (A). (C) $[\text{Ca}^{2+}]_{\text{er}}$ and $[\text{Ca}^{2+}]_{\text{cyt}}$ in the absence of extracellular Ca^{2+} (2 mM EGTA). Data are representative of 13 experiments. (D) Second Ca^{2+} oscillation in (C) shown on expanded time scale. (E) Initial Ca^{2+} oscillation in (C) shown on expanded time scale. (F,G) Averaged and normalized time courses of the first Ca^{2+} oscillations (F), and the second and third Ca^{2+} oscillations (G) in the absence of extracellular Ca^{2+} . Data are mean \pm s.e.m. ($n = 13$).

Abad *et al*, 2004) yielded a K_d of 80 nM (supplementary Fig 3 online). When expressed in HeLa cells, inverse-pericam2-*mt* was localized within tubular structures in the cytoplasm and colocalized with a mitochondrial marker dye (supplementary Fig 4 online).

Fig 3A,C shows the simultaneous measurements of $[\text{Ca}^{2+}]_{\text{cyt}}$ and $[\text{Ca}^{2+}]_{\text{mt}}$ using fura-2 and inverse-pericam2-*mt*, respectively, during histamine-induced Ca^{2+} oscillations in the presence and absence of extracellular Ca^{2+} . There was a rapid increase in $[\text{Ca}^{2+}]_{\text{mt}}$ at the onset of the first $[\text{Ca}^{2+}]_{\text{cyt}}$ spike, and a sinusoidal change in $[\text{Ca}^{2+}]_{\text{mt}}$ followed in phase with the subsequent Ca^{2+}

oscillations on top of the gradual decay, as reported previously (Filippin *et al*, 2003). With a closer look at the time course, one notices a phase difference between the two measurements. At the onset of the initial $[\text{Ca}^{2+}]_{\text{cyt}}$ spike, $[\text{Ca}^{2+}]_{\text{mt}}$ increased with $[\text{Ca}^{2+}]_{\text{cyt}}$, but it continued to increase even after $[\text{Ca}^{2+}]_{\text{cyt}}$ reached its peak (Fig 3E). Fig 3F shows the average time courses of $[\text{Ca}^{2+}]_{\text{cyt}}$ and $[\text{Ca}^{2+}]_{\text{mt}}$ during the first Ca^{2+} oscillation after a normalization procedure similar to that in Fig 2F. Thus, at the peak $[\text{Ca}^{2+}]_{\text{cyt}}$ only $\sim 56\%$ ($55.5 \pm 11.9\%$, mean \pm s.d., $n = 11$) of the full $[\text{Ca}^{2+}]_{\text{mt}}$ response was reached. After $[\text{Ca}^{2+}]_{\text{cyt}}$ reached its peak, Ca^{2+} influx into mitochondria continued for 9.2 ± 2.4 s

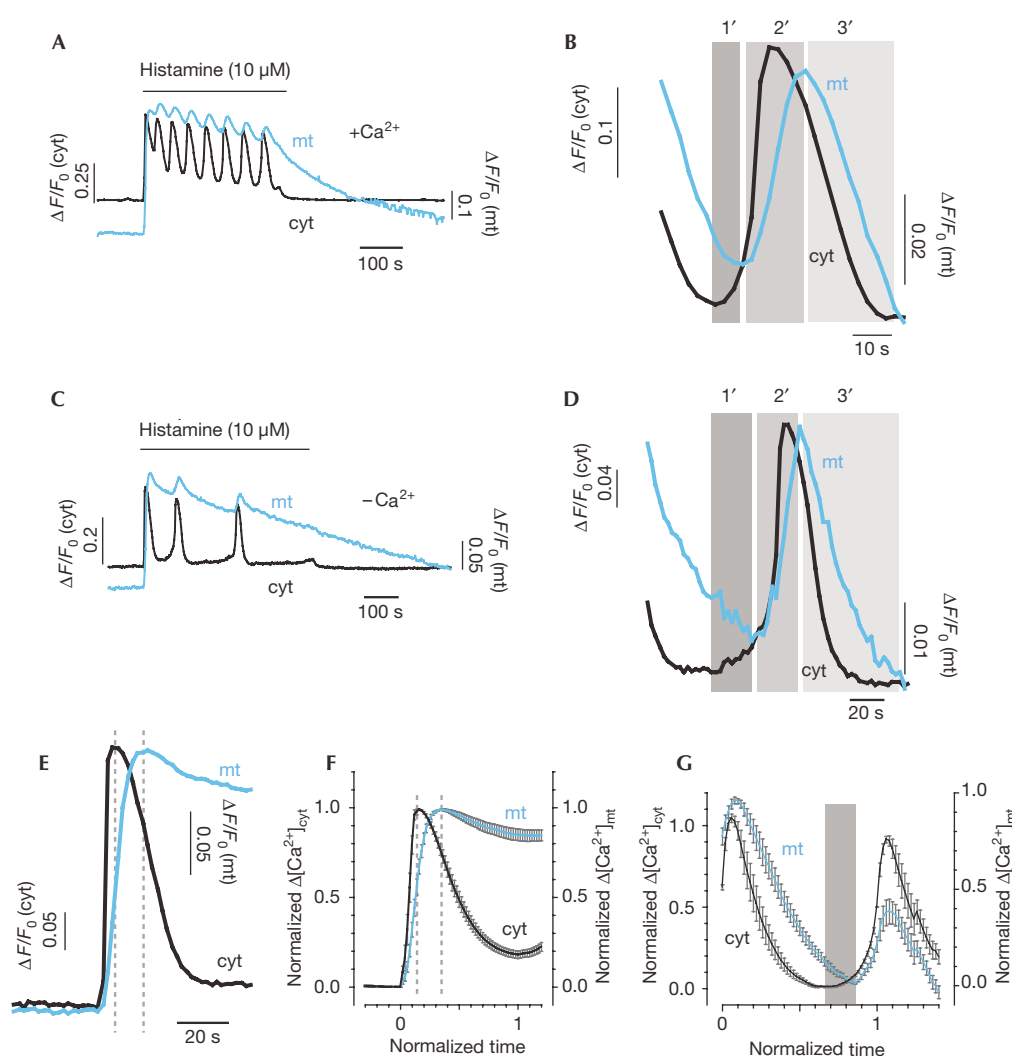


Fig 3 | Phase difference between $[\text{Ca}^{2+}]_{\text{mt}}$ and $[\text{Ca}^{2+}]_{\text{cyt}}$. (A) Simultaneous measurement of $[\text{Ca}^{2+}]_{\text{mt}}$ and $[\text{Ca}^{2+}]_{\text{cyt}}$ using inverse-pericam2-mt and fura-2, respectively, during histamine application in the presence of extracellular Ca^{2+} (2 mM). Data are representative of eight experiments. (B) Expanded time courses of $[\text{Ca}^{2+}]_{\text{mt}}$ and $[\text{Ca}^{2+}]_{\text{cyt}}$ of the fifth Ca^{2+} oscillation in (A). (C) $[\text{Ca}^{2+}]_{\text{mt}}$ and $[\text{Ca}^{2+}]_{\text{cyt}}$ in the absence of extracellular Ca^{2+} (2 mM EGTA). Data are representative of 11 experiments. (D) Second Ca^{2+} oscillation in (C) shown on expanded time scale. (E) Initial Ca^{2+} oscillation in (C) shown on expanded time scale. (F,G) Averaged and normalized time courses of the first Ca^{2+} oscillations (F), and the second and third Ca^{2+} oscillations (G) in the absence of extracellular Ca^{2+} . Data are mean \pm s.e.m. ($n = 11$).

(mean \pm s.d., $n = 11$). This indicates that there is a continuous supply of Ca^{2+} into mitochondria with decreasing $[\text{Ca}^{2+}]_{\text{cyt}}$. As the ER continues to release Ca^{2+} even after $[\text{Ca}^{2+}]_{\text{cyt}}$ reaches its peak (Fig 2E,F), the results indicate that Ca^{2+} is transferred from the ER to mitochondria during the initial Ca^{2+} spike. A similar observation has been reported by previous authors (Szabadkai et al, 2003). The *in vitro* calibration of inverse-pericam2-mt suggests that the peak $[\text{Ca}^{2+}]_{\text{mt}}$ response to histamine is of the order of several hundred nanomolar. This is lower than the previous estimations ($\sim 3\text{--}80\ \mu\text{M}$) derived from measurements in HeLa cells using aequorin, ratiometric pericam and Rhod-2 (Collins et al, 2001; Filippin et al, 2003; Szabadkai et al, 2003), although the present estimation is similar to the value obtained in adrenal chromaffin cells (Babcock et al, 1997). There are difficulties in estimating absolute values of $[\text{Ca}^{2+}]_{\text{mt}}$ because of

the possible uncertainties in applying *in vitro* calibration to *in situ* $[\text{Ca}^{2+}]_{\text{mt}}$. Indeed, it was reported that *in vitro* K_d of ratiometric pericam was about ninefold lower than estimated *in vivo* K_d (Filippin et al, 2003).

During the second and subsequent Ca^{2+} oscillations, we noted three phases (Fig 3B,D). In phase 1' (from the bottom $[\text{Ca}^{2+}]_{\text{cyt}}$ to the initiation of Ca^{2+} uptake by mitochondria), $[\text{Ca}^{2+}]_{\text{cyt}}$ increased gradually to form the foot of Ca^{2+} oscillation. $[\text{Ca}^{2+}]_{\text{mt}}$ decreased (that is, mitochondria were releasing Ca^{2+}) during phase 1'. In phase 2' (the rise phase of $[\text{Ca}^{2+}]_{\text{mt}}$), $[\text{Ca}^{2+}]_{\text{cyt}}$ increased but reached a peak before the peak of $[\text{Ca}^{2+}]_{\text{mt}}$. In late phase 2', $[\text{Ca}^{2+}]_{\text{mt}}$ increased even though $[\text{Ca}^{2+}]_{\text{cyt}}$ decreased. In phase 3' (from the peak $[\text{Ca}^{2+}]_{\text{mt}}$ to the bottom $[\text{Ca}^{2+}]_{\text{cyt}}$), both $[\text{Ca}^{2+}]_{\text{cyt}}$ and $[\text{Ca}^{2+}]_{\text{mt}}$ decreased. The timing of phases 1'–3' in mitochondrial Ca^{2+} transients well corresponded to that of phases

1–3 in ER Ca^{2+} transients. We also obtained the average time courses of $[\text{Ca}^{2+}]_{\text{cyt}}$ and $[\text{Ca}^{2+}]_{\text{mt}}$ after a normalization procedure similar to that in Fig 2G. Again, the features of the typical data are retained in the compiled data, and $[\text{Ca}^{2+}]_{\text{mt}}$ decreased when $[\text{Ca}^{2+}]_{\text{cyt}}$ began to increase in phase 1' (Fig 3G).

Effects of interference with mitochondrial functions

The comparison of the results shown in Figs 2,3 suggests that Ca^{2+} shuttles back and forth between the ER and mitochondria, and that Ca^{2+} regulation by mitochondria is critically involved in the generation of Ca^{2+} oscillations. We further tested this possibility by disrupting the mitochondrial functions in the following experiments. We first reduced mitochondrial membrane potential using oligomycin and FCCP to inhibit Ca^{2+} uptake by the organelle. On application of histamine, $[\text{Ca}^{2+}]_{\text{cyt}}$ increased without oscillations (Fig 4A). $[\text{Ca}^{2+}]_{\text{er}}$ decreased and remained at a decreased level. $[\text{Ca}^{2+}]_{\text{mt}}$ hardly showed an increase. Therefore, it seems that the recycling of Ca^{2+} released from the ER is hampered in the absence of mitochondrial Ca^{2+} uptake.

We then inhibited the release of Ca^{2+} from mitochondria by inhibiting the mitochondrial $\text{Na}^+/\text{Ca}^{2+}$ exchanger. Following activation with histamine, Ca^{2+} is released from the ER, and both $[\text{Ca}^{2+}]_{\text{cyt}}$ and $[\text{Ca}^{2+}]_{\text{mt}}$ increased in the presence of an inhibitor of the $\text{Na}^+/\text{Ca}^{2+}$ exchanger, CGP-37157, as was the case under the control conditions (Fig 4B). However, the release of Ca^{2+} from mitochondria was greatly inhibited. Again, there were no Ca^{2+} oscillations and $[\text{Ca}^{2+}]_{\text{er}}$ remained at a decreased level. The application of CGP-37157 was initiated 10 min before the measurements, but there was no sign of significant reduction in the ER Ca^{2+} content or in the release of ER Ca^{2+} following application of histamine. This suggests that CGP-37157 had no appreciable effect on SERCA activity. We also examined the possible effect of CG-37157 on histamine-induced IP_3 production using an IP_3 indicator GFP-PHD (Hirose *et al*, 1999). We found no significant effect of the drug on IP_3 production (supplementary Fig 5 online).

$[\text{Ca}^{2+}]_{\text{mt}}$ showed sinusoidal changes, but it gradually decreased with time, probably owing to a gradual transfer of Ca^{2+} to the ER or extracellular space (Fig 3A,C). If Ca^{2+} release from mitochondria was necessary for priming each Ca^{2+} oscillation (except for the initial Ca^{2+} spike), the Ca^{2+} oscillation should have stopped after $[\text{Ca}^{2+}]_{\text{mt}}$ was depleted. We therefore observed Ca^{2+} oscillations in the absence of extracellular Ca^{2+} until $[\text{Ca}^{2+}]_{\text{mt}}$ approached the pre-stimulation level. Indeed, the Ca^{2+} oscillation pattern became irregular with the decrease in $[\text{Ca}^{2+}]_{\text{mt}}$, and finally Ca^{2+} oscillation stopped (Fig 4C). Conversely, $[\text{Ca}^{2+}]_{\text{er}}$ between the Ca^{2+} oscillations gradually increased with time ($n=13$; Fig 2C). These results are consistent with the notion that mitochondrial Ca^{2+} regulation has a pivotal role in the generation of Ca^{2+} oscillations.

The model

The mechanism of the initiation of agonist-induced Ca^{2+} spikes has been studied extensively by several authors and found to show the importance of the regenerative release of Ca^{2+} from the ER (Iino *et al*, 1993; Bootman *et al*, 1997; Marchant & Parker, 2001; Miyakawa *et al*, 2001). The present measurements are consistent with such notion with regard to the very first Ca^{2+} oscillation, but show more features of subsequent oscillations. In the second and

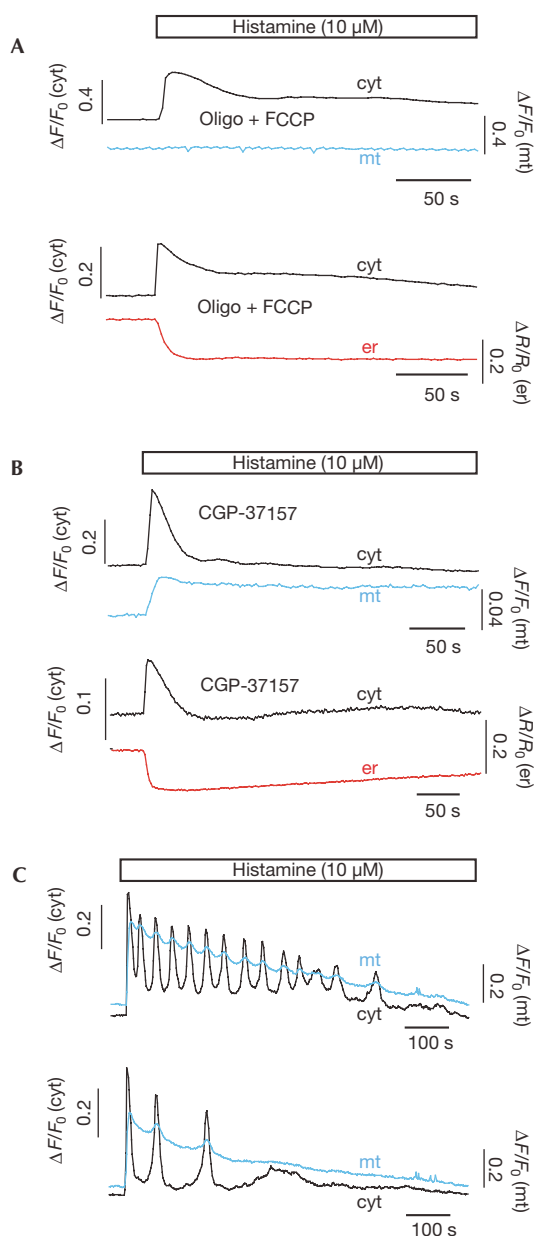


Fig 4 | Importance of mitochondrial function in Ca^{2+} oscillation. (A) Effect of mitochondrial depolarizing inhibitors (oligomycin (10 $\mu\text{g}/\text{ml}$) plus FCCP (5 μM)) on histamine-induced changes in $[\text{Ca}^{2+}]_{\text{cyt}}$ and $[\text{Ca}^{2+}]_{\text{mt}}$ (upper panel), and $[\text{Ca}^{2+}]_{\text{cyt}}$ and $[\text{Ca}^{2+}]_{\text{er}}$ (lower panel). (B) Effect of mitochondrial $\text{Na}^+/\text{Ca}^{2+}$ exchanger inhibitor (CGP-37157, 10 μM) on histamine-induced changes in $[\text{Ca}^{2+}]_{\text{cyt}}$ and $[\text{Ca}^{2+}]_{\text{mt}}$ (upper panel), and $[\text{Ca}^{2+}]_{\text{cyt}}$ and $[\text{Ca}^{2+}]_{\text{er}}$ (lower panel). The application of mitochondrial inhibitors was initiated 10 min before the measurements. (C) During prolonged histamine application in the absence of extracellular Ca^{2+} , $[\text{Ca}^{2+}]_{\text{mt}}$ gradually decreased and at the same time $[\text{Ca}^{2+}]_{\text{cyt}}$ oscillation stopped. All data were obtained in the absence of extracellular Ca^{2+} , and are representative of five experiments.

subsequent Ca^{2+} oscillations, $[\text{Ca}^{2+}]_{\text{cyt}}$ increased before the initiation of Ca^{2+} release from the ER even in the absence of extracellular Ca^{2+} . Thus, we have to consider the involvement

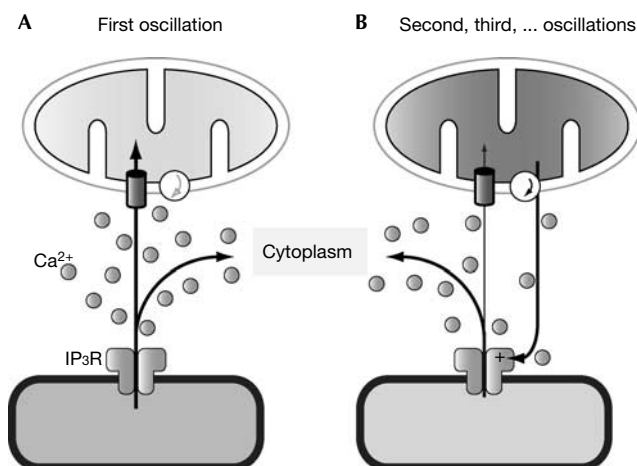


Fig 5 | Schematic drawings of Ca^{2+} regulation by endoplasmic reticulum and mitochondria during Ca^{2+} oscillations. (A) The first Ca^{2+} oscillation is generated by Ca^{2+} release from the endoplasmic reticulum (ER) by means of inositol 1,4,5-trisphosphate receptor (IP₃R). A considerable fraction of Ca^{2+} released from the ER is taken up by mitochondria. (B) The second and subsequent Ca^{2+} oscillations are initiated by the Ca^{2+} release from mitochondria, which then triggers regenerative Ca^{2+} release from the ER. Mitochondrial Ca^{2+} is partially reloaded. The sequence is repeated until mitochondrial Ca^{2+} is depleted. In both (A,B), the regenerative Ca^{2+} -induced Ca^{2+} release mechanism underlies the upstroke of each Ca^{2+} oscillation (not shown).

of another Ca^{2+} store. Indeed, several previous reports have indicated the role of mitochondrial in the cytoplasmic Ca^{2+} buffering and in the generation of Ca^{2+} waves and oscillations (Jouaville *et al*, 1995; Babcock *et al*, 1997; Falcke *et al*, 1999; also see Wagner *et al*, 1998). We have now directly visualized Ca^{2+} concentrations in mitochondria as well as in the ER. Our results indicate that Ca^{2+} shuttles between the ER and mitochondria along with the Ca^{2+} oscillations, and that the following sequence of events drives Ca^{2+} oscillations. The IP₃-induced Ca^{2+} release from the ER is essential for the initiation of the first Ca^{2+} spike, during which mitochondria are loaded with Ca^{2+} released from the ER (Fig 5A). During the second and subsequent Ca^{2+} oscillations, the $\text{Na}^+/\text{Ca}^{2+}$ exchanger-mediated Ca^{2+} release from mitochondria supplies the primer Ca^{2+} to generate the foot of each Ca^{2+} oscillation. When the foot reaches a threshold, it then activates IP₃R, causing the regenerative release of Ca^{2+} from the ER (Fig 5B).

It has been shown that the mitochondrial matrix buffers Ca^{2+} reversibly with an effective Ca^{2+} -binding ratio of $\sim 4,000$, which is 40 times the Ca^{2+} -binding ratio of the cytoplasm (Babcock *et al*, 1997). Mitochondria occupy $\sim 12\%$ of the volume of HeLa cells (Sesso *et al*, 2004). Therefore, mitochondrial Ca^{2+} is highly buffered and its release should be able to increase $[\text{Ca}^{2+}]_{\text{cyt}}$. Furthermore, the inhibition of mitochondrial Ca^{2+} release either by inhibitors or by Ca^{2+} depletion interfered with Ca^{2+} oscillations (Fig 4). Taken together, both the ER and mitochondria seem to have important roles in Ca^{2+} regulation during Ca^{2+} oscillations, although we do not exclude the possibility that non-ER Ca^{2+} stores, such as the Golgi apparatus (Missiaen *et al*, 2004), may also make further contributions. Thus, a mitochondrial

dysfunction is expected to have a significant impact on Ca^{2+} oscillation dynamics.

METHODS

Indicators. The complementary DNA fragments encoding CFP-CaM7-er, M13-Citrine-er and inverse-pericam2 were constructed on the basis of pcDNA3-YC4.1er and pcDNA3-inverse-pericam (gift from Dr A. Miyawaki, RIKEN, Wako, Japan). Details of mutagenesis, generation of recombinant proteins and retroviruses are available in the supplementary information online.

Fluorescence imaging. HeLa cells transduced with retroviruses encoding the indicators and cultured in glass-bottomed dish (MatTek) were loaded at room temperature ($23\text{ }^\circ\text{C}$ – $25\text{ }^\circ\text{C}$) with $5\text{ }\mu\text{M}$ indo-5F AM or fura-2 AM in physiological salt solution containing 150 mM NaCl, 4 mM KCl, 2 mM CaCl_2 , 1 mM MgCl_2 , 5.6 mM glucose and 25 mM Hepes (pH 7.4). Pairs of fluorescence images at 480 and 535 nm were simultaneously captured using an inverted microscope (IX70; Olympus, Japan) equipped with a $\times 60$ objective (NA 1.2) and an image acquisition system (W-View; Hamamatsu Photonics, Japan) at a rate of one frame per 2 s. The excitation wavelengths were 346 nm for indo-5F, 434 nm for split-YC7.3er cameleon, 380 nm for fura-2 and 490 nm for inverse-pericam2-mt.

For the simultaneous imaging of $[\text{Ca}^{2+}]_{\text{cyt}}$ (indo-5F) and $[\text{Ca}^{2+}]_{\text{er}}$ (split-YC7.3er cameleon), fluorescence images at 480 nm from indo-5F with 346 nm excitation represent $[\text{Ca}^{2+}]_{\text{cyt}}$ and those at 535 nm fluorescence were divided by the corresponding images at 480 nm on a pixel-to-pixel basis to obtain the fluorescent resonance energy transfer efficiency of split-YC7.3er cameleon at 434 nm excitation. For the simultaneous imaging of $[\text{Ca}^{2+}]_{\text{cyt}}$ (fura-2) and $[\text{Ca}^{2+}]_{\text{mt}}$ (inverse-pericam2-mt), fluorescence images at 535 nm from either inverse-pericam2-mt (490 nm excitation) or fura-2 (380 nm excitation) were alternately obtained. **Supplementary information** is available at *EMBO reports* online (<http://www.emboports.org>).

ACKNOWLEDGEMENTS

This work was supported by Grants in Aid for Scientific Research and partly by Advanced and Innovative Research Program in Life Science from the Ministry of Education, Culture, Sports, Science and Technology, Japan.

REFERENCES

- Abad MF, Di Benedetto G, Magalhaes PJ, Filippin L, Pozzan T (2004) Mitochondrial pH monitored by a new engineered green fluorescent protein mutant. *J Biol Chem* **279**: 11521–11529
- Babcock DF, Herrington J, Goodwin PC, Park YB, Hille B (1997) Mitochondrial participation in the intracellular Ca^{2+} network. *J Cell Biol* **136**: 833–844
- Berridge MJ, Lipp P, Bootman MD (2000) The versatility and universality of calcium signalling. *Nat Rev Mol Cell Biol* **1**: 11–21
- Bezprozvanny I, Watras J, Ehrlich BE (1991) Bell-shaped calcium-response curves of Ins(1,4,5) P_3 - and calcium-gated channels from endoplasmic reticulum of cerebellum. *Nature* **351**: 751–754
- Bootman MD, Berridge MJ, Lipp P (1997) Cooking with calcium: the recipes for composing global signals from elementary events. *Cell* **91**: 367–373
- Collins TJ, Lipp P, Berridge MJ, Bootman MD (2001) Mitochondrial Ca^{2+} uptake depends on the spatial and temporal profile of cytosolic Ca^{2+} signals. *J Biol Chem* **276**: 26411–26420
- Clapham DE (1995) Calcium signaling. *Cell* **80**: 259–268
- De Koninck P, Schulman H (1998) Sensitivity of CaM kinase II to the frequency of Ca^{2+} oscillations. *Science* **279**: 227–230
- Dolmetsch RE, Xu K, Lewis RS (1998) Calcium oscillations increase the efficiency and specificity of gene expression. *Nature* **392**: 933–936

- Falcke M, Hudson JL, Camacho P, Lechleiter JD (1999) Impact of mitochondrial Ca²⁺ cycling on pattern formation and stability. *Biophys J* **77**: 37–44
- Filippin L, Magalhaes PJ, Di Benedetto G, Colella M, Pozzan T (2003) Stable interactions between mitochondria and endoplasmic reticulum allow rapid accumulation of calcium in a subpopulation of mitochondria. *J Biol Chem* **278**: 39224–39234
- Hirose K, Kadowaki S, Tanabe M, Takeshima H, Iino M (1999) Spatio-temporal dynamics of inositol 1,4,5-trisphosphate that underlies complex Ca²⁺ mobilization patterns. *Science* **284**: 1527–1530
- Iino M (1990) Biphasic Ca²⁺ dependence of inositol 1,4,5-trisphosphate-induced Ca release in smooth muscle cells of the guinea pig *Taenia caeci*. *J Gen Physiol* **95**: 1103–1122
- Iino M, Yamazawa T, Miyashita Y, Endo M, Kasai H (1993) Critical intracellular Ca²⁺ concentration for all-or-none Ca²⁺ spiking in single smooth muscle cells. *EMBO J* **12**: 5287–5291
- Jouaville LS, Ichas F, Holmuhamedov EL, Camacho P, Lechleiter JD (1995) Synchronization of calcium waves by mitochondrial substrates in *Xenopus laevis* oocytes. *Nature* **377**: 438–441
- Li W, Llopis J, Whitney M, Zlokarnik G, Tsien RY (1998) Cell-permeant caged Ins P₃ ester shows that Ca²⁺ spike frequency can optimize gene expression. *Nature* **392**: 936–941
- Marchant JS, Parker I (2001) Role of elementary Ca²⁺ puffs in generating repetitive Ca²⁺ oscillations. *EMBO J* **20**: 65–76
- Missiaen L et al (2004) Calcium release from the Golgi apparatus and the endoplasmic reticulum in HeLa cells stably expressing targeted aequorin to these compartments. *Cell Calcium* **36**: 479–487
- Miyakawa T, Mizushima A, Hirose K, Yamazawa T, Bezprozvanny I, Kurosaki T, Iino M (2001) Ca²⁺-sensor region of IP₃ receptor controls intracellular Ca²⁺ signaling. *EMBO J* **20**: 1674–1680
- Miyawaki A, Llopis J, Heim R, McCaffery JM, Adams JA, Ikura M, Tsien RY (1997) Fluorescent indicators for Ca²⁺ based on green fluorescent proteins and calmodulin. *Nature* **388**: 882–887
- Nagai T, Sawano A, Park ES, Miyawaki A (2001) Circularly permuted green fluorescent proteins engineered to sense Ca²⁺. *Proc Natl Acad Sci USA* **98**: 3197–3202
- Oancea E, Meyer T (1998) Protein kinase C as a molecular machine for decoding calcium and diacylglycerol signals. *Cell* **95**: 307–318
- Rizzuto R, Pinton P, Carrington W, Fay FS, Fogarty KE, Lifshitz LM, Tuft RA, Pozzan T (1998) Close contacts with the endoplasmic reticulum as determinants of mitochondrial Ca²⁺ responses. *Science* **280**: 1763–1766
- Sesso A et al (2004) Morphology of mitochondrial permeability transition: morphometric volumetry in apoptotic cells. *Anat Rec A Discov Mol Cell Evol Biol* **281**: 1337–1351
- Szabadkai G, Simoni AM, Rizzuto R (2003) Mitochondrial Ca²⁺ uptake requires sustained Ca²⁺ release from the endoplasmic reticulum. *J Biol Chem* **278**: 15153–15161
- Tomida T, Hirose K, Takizawa A, Shibasaki F, Iino M (2003) NFAT functions as a working memory of Ca²⁺ signals in decoding Ca²⁺ oscillation. *EMBO J* **22**: 3825–3832
- Wagner J, Li YX, Pearson J, Keizer J (1998) Simulation of the fertilization Ca²⁺ wave in *Xenopus laevis* eggs. *Biophys J* **75**: 2088–2097